Science & Technology Development Journal, 24(SI1):SI79-SI84

Open Access Full Text Article

Research Article

Insight into the interaction mechanism of thioflavin-t with an amyloid beta (1-42) by the docking method

N. Q. Thai[1], H. Q. Linh[2,*]

Use your smartphone to scan this QR code and download this article

ABSTRACT

Alzheimer's disease is associated with a progressive intracerebral accumulation of amyloid beta (Aβ) peptides, which have different numbers of amino acids, but Aβ40 and Aβ42 are the most abundant *in vivo*. However, Aβ42 is more toxic than Aβ40. Thioflavin-T has been used in research to investigate amyloid beta formation, but the interaction mechanism remains unclear. In this study, using the docking method, we calculated the binding between thioflavin-T and aggregations of Aβ42, including fibril, tetramer, and dimer Aβ42. The results show that thioflavin-T binds to fibrils more strongly than soluble oligomers. The binding mechanism depends on the conformations of the assembly structures.

Key words: Alzheimer's disease, Aβ40, and Aβ42, docking method, thioflavin-T, binding affinity

[1]*Faculty of Natural Sciences Teacher Education, Dong Thap University, Dong Thap, Vietnam*

[2]*Faculty of Applied Science, Ho Chi Minh City University of Technology, National University Ho Chi Minh city, Vietnam*

Correspondence

H. Q. Linh, Faculty of Applied Science, Ho Chi Minh City University of Technology, National University Ho Chi Minh city, Vietnam

Email: huynhqlinh@hcmut.edu.vn

History

- Received: 2022-02-23
- Accepted: 2022-05-02
- Published: 2022-05-11

DOI : 10.32508/stdj.v24iSI1.3904

Check for updates

Copyright

© VNUHCM Press. This is an open-access article distributed under the terms of the Creative Commons Attribution 4.0 International license.

INTRODUCTION

Among elderly people, the most common kind of neurodegenerative disease is Alzheimer's disease (AD)[1]. There are dozens of hypotheses about its causes. However, recent experimental evidence strongly supports the amyloid cascade hypothesis (molecular imbalance)[1], which is based on an imbalance between the production and clearance of Aβ peptides in the brain[2]. Amyloid beta (Aβ) peptides are produced from amyloid precursor protein (APP) by the activity of enzyme secretases such as β- and γ-secretase[3]. Aβ peptides have different numbers of amino acids, but Aβ40 and Aβ42 are most abundant *in vivo*[4,5], and Aβ42 is more toxic than Aβ40.

In drug discovery and development, mainly computational simulations are used to optimize promising new compounds by estimating their binding affinity to proteins, linear correlations between kinetic rates and binding affinity constants[6,7], and predict drug-target binding kinetic parameters[8]. For over a decade, researchers have focused on the fundamental mechanism of the interaction between thioflavin-T and amyloid fibrils. In 1959, Vassar and Culling, who were the first to present the unity of the benzothiazole dye thioflavin-T, demonstrated the potential of using fluorescence microscopy for amyloid fibril diagnosis and markers of amyloid in histology[9], and later, Naiki *et al* and LeVin were clearly explained to characterize the fluorescence spectra and binding properties of thioflavin-T. They demonstrated that when thioflavin-T binds to amyloid fibrils, thioflavin-T gives a fluorescence signal with an excitation maximum at 450 nm and an emission maximum at 482 nm[10] and only originates from the dye bound to amyloid fibrils[10,11]. Thioflavin-T binds to the side chain channels along the long axis of amyloid fibrils. *In vitro*, the inhibition constant (IC50) of thioflavin-T with amyloid fibrils was measured at 890 $\pm$ 92 nM[12]. The relationship between IC50 and energy free binding was ΔE_{bind} = RTln(IC50), where the gas constant R = 1.987 $\times$ 10^{-}3 kcal.mol^{-1}, T = 300 K, and the inhibition constant IC50 was measured in mol. However, most of these studies were based on a single model structure for fibrils and did not consider the influence of various aggregation states of amyloid beta, such as dimers, tetramers, and many different fibril shapes. In this study, we attempted to gain insight into the interaction mechanism of thioflavin-T and the aggregation states of amyloid beta (1-42) peptide. The binding affinity of thioflavin-T to several targets, including dimer, tetramer, two conformations 2MXU and 2NAO of fibril Aβ42, will be investigated. Using the docking simulation, we obtained the binding site and other quantities, such as the binding affinity, the number of hydrogen bonds (HB), and nonbond contacts (NBCs) of thioflavin-T with targets. Thioflavin-T binds to fibrils more strongly than oligomers. The binding mechanism depends on the conformations of assembly states.

MATERIAL AND METHODS

Initial structures

In this study, we chose Aβ42 because many studies have shown that Aβ42 is more toxic than Aβ40,

Cite this article : Thai N Q, Linh H Q. **Insight into the interaction mechanism of thioflavin-t with an amyloid beta (1-42) by the docking method**. *Sci. Tech. Dev. J.;* 24(SI1):SI79-SI84.

and this isoform is the main component of amyloid plaques. The solid-state NMR crystal structures of the truncated fragment Aβ7-42 with PDB code 2MXU [13], which has residues and chains more than the 2BEG structure, and full length Aβ1-42 with PDB code 2NAO [14] will be used for docking. For dimers, the model developed in [15] will be utilized. For tetramers, we employed the model obtained by our group using MD simulation [16]. All targets are shown in Figure 1.

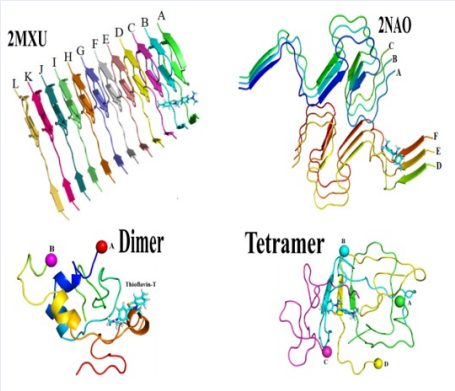

Figure 1: The structures of amyloid beta aggregates used in this work. Positions of thioflavin-T in the best docking mode for the targets.

Thioflavin-T structure

The atomic structure of thioflavin-T was obtained from the large PubChem [17] database (https://pubchem.ncbi.nlm.nih.gov) with CID 16954 (4-(3,6-dimethyl-1,3-benzothiazole-3-ium-2-yl)-N,N-dimethylaniline). The 3D and 2D structures are shown in Figure 2. Information about the chemical and physical properties of thioflavin-T is presented in Table 1.

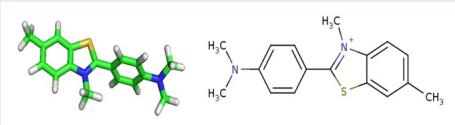

Figure 2: The 3D (left) and 2D (right) structures of thioflavin-T.

Docking method

The PDBQT files of thioflavin-T and the amyloid beta targets (2MXU, 2NAO, dimer, tetramer) were prepared by AutoDock Tool version 1.5.4 [18]. The docking simulations of thioflavin-T to targets were performed using AutoDock Vina version 1.1 [19]. For the global search, the exhaustiveness was set to 800, which is high enough to achieve reliable results.

Data analysis

The hydrogen bond (HB) is formed when the D (donor)-A (acceptor) atom distance $\leq$ 3.5 Å, H (hydro)-A distance 2.7 $\leq$ Å, and D-H-A angle $\geq$ 135 degrees. If the distance between the centers of mass of the ligand and the side chain of one receptor residue is within 0.65 nm, then we assume that a nonbonded contact (NBC) is formed between the protein and ligand. The binding energy is the binding affinity of the best docking modes, which is the sum of the intermolecular forces acting upon the receptor–ligand complex.

RESULTS AND DISCUSSION

Protein structure and box sizes

Figure 1 shows the cartoon representation of these targets. Because the binding site of thioflavin-T in these targets was not a priori known, a sufficiently large grid box was created around the detected binding pocket with a spacing of 0.375 Å. The box sizes and center of boxes are presented in Table 2. A large grid box allows the ligand to traverse a larger conformational space on the protein surface and perform the blind docking process.

Docking scores and best docking poses

The positions of thioflavin-T in binding to the targets in the lowest binding energy mode obtained from docking simulations are shown in Figure 1. The results showed that thioflavin-T is located inside the targets. Thioflavin-T is near amino acids Gly33 of chain C and His14 and Gly33 of chain B (2MXU). For 2NAO, thioflavin-T is linked near His6 of chain E and Tyr10 of chain D. For dimer, thioflavin-T binds to residues Phe64 of chain B and Ala22 of chain A. Meanwhile, thioflavin-T approached amino acid Val123 of chain C and Leu160 of chain D for tetramer target.

The binding energies, number of hydrogen bonds (HBs), and nonbonded contacts (NBCs) of thioflavin-T with targets were computed and obtained in the best docking modes, as shown in Table 3 and Figure 3.

In the best docking modes, the binding energies of thioflavin-T and 2MXU were slightly stronger than that of 2NAO, which were -6.6 and -6.2 kcal.mol^{-1}, respectively (Table 3). This result suggests that thioflavin-T favors binding the one-fold symmetry

Table 1: Chemical and physical properties of thioflavin-T.

Molecular weight	Hydrogen bond donor count	Hydrogen bond acceptor count	Rotatable bond count
318.9	0	3	2
Topological polar surface area	Heavy atom count	Formal charge	Exact Mass
35.4 $Å^2$	21	0	318.095745

Table 2: The box sizes of complexes in this study.

Target	Size box (Å)	Center of box (Å)
2MXU	70 x 60 x 60	(-0.05, 0.02, 0.07)
2NAO	40 x 70 x 70	(15.61, 30.94, -33.27)
Dimer	45 x 40 x 40	(32.66, 35.48, 37.85)
Tetramer	50 x 70 x 60	(0.09, -0.16, -0.04)

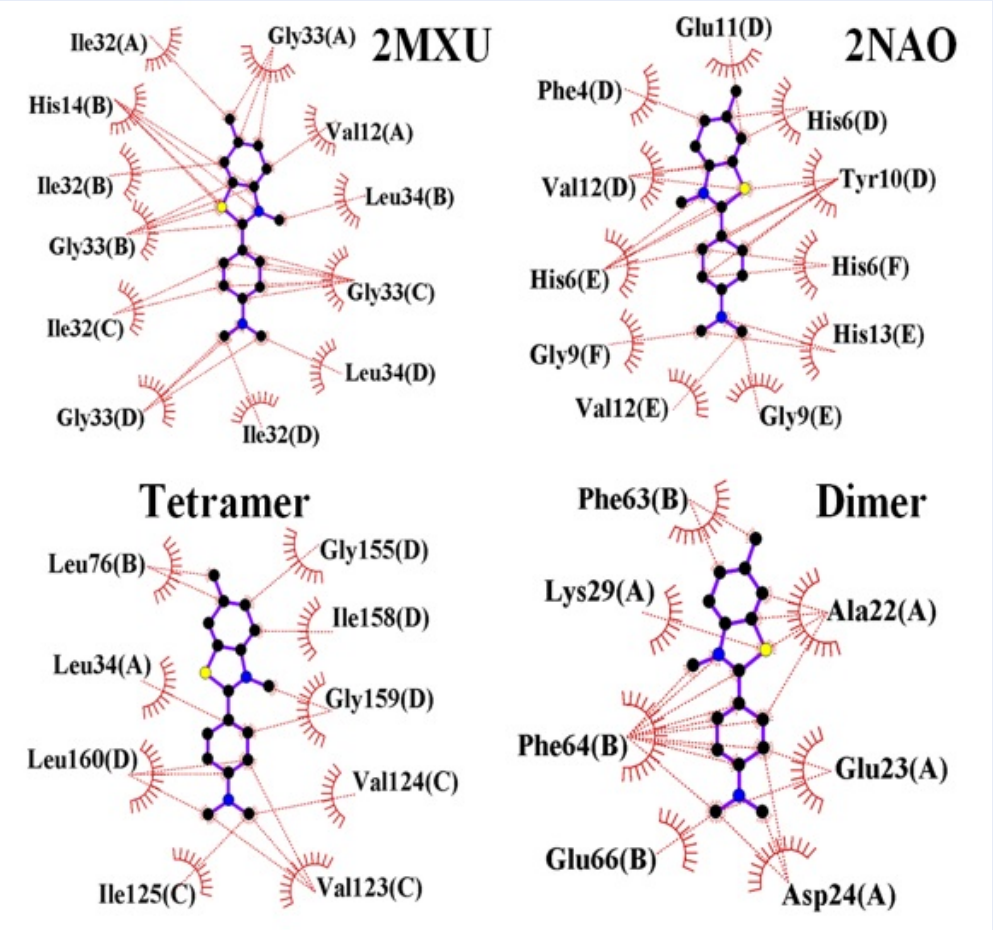

Figure 3: Nonbonded contacts of thioflavin-T with fibrils (2MXU, 2NAO), tetramer, dimer in the best docking mode. The results are shown in Ligplot version 4.5.3.

Table 3: The binding energies, number of HBs, and number of NBCs for thioflavin-T and targets.

Targets	HB	NBC	Binding energy (ΔE_{bind}, kcal.mol^{-1})
2MXU	0	12	-6.6
2NAO	0	11	-6.2
Tetramer	0	9	-5.6
Dimer	0	7	-5.3

fibril structure (2MXU) over the twofold symmetry fibril (2NAO). This can come from the large distance between Thioflavin-T and chains in the other branch of the fibril structure because Thioflavin-T binds to 3 chains in one branch of the structure. However, in the 2MXU structure, the chains arrange in one row, which facilitates the small distance between Thioflavin and the chains of the fibril.

In the case of tetramers and dimers, the binding energies are higher than those of fibrils, which are approximately -5.4 kcal.mol^{-1}. This result can be explained by the fact that the oligomer structures are more compact than fibrils, which makes it harder for thioflavin-T to bind deep inside the structure[16]. Therefore, the binding energies of thioflavin-T and the oligomer are weaker than those of mature fibrils.

The interaction mechanism of thioflavin-T and aggregated forms of Aβ42 depends on assembly states

Table 3 shows that thioflavin-T has no HBs with targets, as is evident from Figure 3, because thioflavin-T has no acceptor atoms such as oxygen or nitrogen. This result suggests that hydrogen bonds have a negligible effect on the interaction between thioflavin-T and aggregations of Aβ42. To confirm the predicted results, more detailed studies and more precise computational methods are needed, such as the molecular mechanics Poisson-Boltzmann surface area (MM-PBSA).

Thioflavin-T has 12 and 11 nonbonded contacts with the fibrillar structures 2MXU and 2NAO, respectively. Meanwhile, the thioflavin-T and tetramer complex has NBCs (9), which are larger than dimers (7 NBCs). Overall, the binding energies are in good agreement with NBCs (Tables 3 and 4). The 2MXU + thioflavin-T complex has the lowest binding energy (-6.6 kcal.mol^{-1}) and forms the largest number of NBCs. In addition, 2NAO has 11 NBCs with ΔE_{bind} = -6.2 kcal.mol^{-1}, and the tetramer has 9 NBCs with ΔE_{bind} = -5.7 kcal.mol^{-1}. In the case of dimer, which has the weakest binding energy (ΔE_{bind} = -5.3 kcal.mol^{-1}), it is appropriate with the smallest number of NBCs (NBC = 7). These results show that the nonbonded contact network is much richer than the hydrogen bond network, implying that hydrogen bonding plays a less important role in the stabilization of receptor–ligand complexes compared to nonbonded bonds.

The total charge of residues that make nonbonded contacts with thioflavin-T is 0 in two fibrillar structures and tetramers, while in dimers, the total charge is -2e. The negative charge value in the dimer case is reasonable because the charge of thioflavin-T is +1e. The 0e charge in fibril conformations and tetramers can come from the arrangement of residues in these structures, leading to charged residues located on the surface of the protein. Therefore, there are no charged binding pockets for thioflavin-T to bind, leading to neural residues at the binding sites of fibrils and tetramers. The total hydrophobicity indexes (Table 4) show that the hydrophobic character of the binding sites depends on the structures of aggregations. Therefore, these results suggest that the binding mechanism between thioflavin-T and Aβ42 aggregations is ruled by the conformations of the Aβ42 aggregations.

CONCLUSION

Using docking simulations, we obtained the binding energies of thioflavin-T and the aggregated forms of amyloid beta dimer, tetramer, and two fibrillar structures. The results show that thioflavin-T favors binding one-fold symmetry of the fibrillar structure of Aβ42 over other forms because the binding energy of 2MXU and thioflavin-T is the lowest. The soluble oligomers, such as dimers and tetramers, have weaker binding energies than mature fibrils.

The nonbonded contacts dominate over hydrogen bonds in the interaction between thioflavin-T and aggregates of Aβ42. Furthermore, the neutral residues of amyloid play an important role in the nonbonded contacts in fibrils and tetramers, while in dimers, the charge of residues in the binding site is -2e. These results suggest that the binding mechanism is ruled by conformations.

Table 4: Amyloid beta residues having nonbonded contact with thioflavin-T. The results were obtained from the best docking modes of thioflavin-T and its targets. The characters in brackets refer to chains of the protein structures.

Target	NBCs	Amino acids	Total charge (e)	Total hydrophobicity[20]
2MXU	12	Gly33(A), Val12(A), Leu34(B), Gly33(C), Leu34(D), Ile32(D), Gly33(D), Ile32(C), Gly33(B), Ile32(B), His14(B), Ile32(A)	0	26.6
2NAO	11	Glu11(D), His6(D), Tyr10(D), His6(F), His13(E), Gly9(E), Val12(E), Gly9(F), His6(E), Val12(D), Phe4(D)	0	-1.6
Tetramer	9	Gly155(D), Ile158(D), Gly159(D), Val124(C), Val123(C), Ile125(C), Leu160(D), Leu34(A), Leu(B)	0	28.8
Dimer	7	Phe63(B), Ala22(A), Glu23(A), Asp24(A), Glu66(B), Phe64(B), Lys29(A)	-2	4.6

CONFLICTS OF INTEREST

The authors declare no competing financial interest.

AUTHOR CONTRIBUTIONS

N. Q. Thai and H. Q. Linh analyzed the results. N. Q. Thai and H. Q. Linh wrote the paper.

ACKNOWLEDGMENT

This research is supported by the project B2019.SPD.03.

REFERENCES

1. Hardy J, Selkoe DJ. The amyloid hypothesis of Alzheimer's disease: progress and problems on the road to therapeutics. science. 2002;297(5580):353-6;PMID: 12130773. Available from: https://doi.org/10.1126/science.1072994.
2. Selkoe DJ, Hardy J. The amyloid hypothesis of Alzheimer's disease at 25 years. EMBO Molecular Medicine. 2016;8(6):595-608;PMID: 27025652. Available from: https://doi.org/10.15252/emmm.201606210.
3. Murphy MP, LeVine III H. Alzheimer's disease and the amyloid-β peptide. Journal of Alzheimer's Disease. 2010;19(1):311-23;PMID: 20061647. Available from: https://doi.org/10.3233/JAD-2010-1221.
4. Mori H, Takio K, Ogawara M, Selkoe D. Mass spectrometry of purified amyloid beta protein in Alzheimer's disease. Journal of Biological Chemistry. 1992;267(24):17082-6;Available from: https://doi.org/10.1016/S0021-9258(18)41896-0.
5. Roher AE, Lowenson JD, Clarke S, Wolkow C, Wang R, Cotter RJ, et al. Structural alterations in the peptide backbone of beta-amyloid core protein may account for its deposition and stability in Alzheimer's disease. Journal of Biological Chemistry. 1993;268(5):3072-83;Available from: https://doi.org/10.1016/S0021-9258(18)53661-9.
6. Decherchi S, Cavalli A. Thermodynamics and kinetics of drug-target binding by molecular simulation. Chemical Reviews. 2020;120(23):12788-833;PMID: 33006893. Available from: https://doi.org/10.1021/acs.chemrev.0c00534.
7. De Benedetti PG, Fanelli F. Computational modeling approaches to quantitative structure-binding kinetics relationships in drug discovery. Drug Discovery Today. 2018;23(7):1396-406;PMID: 29574212. Available from: https://doi.org/10.1016/j.drudis.2018.03.010.
8. Nunes-Alves A, Kokh DB, Wade RC. Recent progress in molecular simulation methods for drug binding kinetics. Current Opinion in Structural Biology. 2020;64:126-33;PMID: 32771530. Available from: https://doi.org/10.1016/j.sbi.2020.06.022.
9. Vassar PS, Culling C. Fluorescent stains, with special reference to amyloid and connective tissues. Archives of pathology. 1959;68:487-98;.
10. Naiki H, Higuchi K, Hosokawa M, Takeda T. Fluorometric determination of amyloid fibrils in vitro using the fluorescent dye, thioflavine T. Analytical biochemistry. 1989;177(2):244-9;Available from: https://doi.org/10.1016/0003-2697(89)90046-8.
11. Levine III H. Thioflavine T interaction with synthetic Alzheimer's disease β-amyloid peptides: Detection of amyloid aggregation in solution. Protein Science. 1993;2(3):404-10;PMID: 8453378. Available from: https://doi.org/10.1002/pro.5560020312.
12. Klunk WE, Wang Y, Huang G-f, Debnath ML, Holt DP, Mathis CA. Uncharged thioflavin-T derivatives bind to amyloid-beta protein with high affinity and readily enter the brain. Life sciences. 2001;69(13):1471-84;Available from: https://doi.org/10.1016/S0024-3205(01)01232-2.
13. Xiao Y, Ma B, McElheny D, Parthasarathy S, Long F, Hoshi M, et al. A [beta](1-42) fibril structure illuminates self-recognition and replication of amyloid in Alzheimer's disease. Nat Struct Mol Biol. 2015;22(6):499-505;PMID: 25938662. Available from: https://doi.org/10.1038/nsmb.2991.
14. Wälti MA, Ravotti F, Arai H, Glabe CG, Wall JS, Böckmann A, et al. Atomic-resolution structure of a disease-relevant Aβ (1-42) amyloid fibril. Proc Natl Acad Sci USA. 2016;113(34):E4976-E84;PMID: 27469165. Available from: https://doi.org/10.1073/pnas.1600749113.
15. Zhang Y, Hashemi M, Lv Z, Lyubchenko YL. Self-assembly of the full-length amyloid Aβ42 protein in dimers. Nanoscale. 2016;8(45):18928-37;PMID: 27714140. Available from: https://doi.org/10.1039/C6NR06850B.
16. Nguyen HL, Krupa P, Hai NM, Linh HQ, Li MS. Structure and physicochemical properties of the Aβ42 tetramer: Multi-scale molecular dynamics simulations. The Journal of Physical Chemistry B. 2019;123(34):7253-69;PMID: 31365254. Available from: https://doi.org/10.1021/acs.jpcb.9b04208.
17. Kim S, Thiessen PA, Bolton EE, Chen J, Fu G, Gindulyte A, et al. PubChem substance and compound databases. Nucleic acids research. 2015;44(D1):D1202-D13;PMID: 26400175. Available from: https://doi.org/10.1093/nar/gkv951.
18. Sanner MF. Python: a programming language for software integration and development. J Mol Graph Model. 1999;17(1):57-61;.
19. Trott O, Olson AJ. AutoDock Vina: improving the speed and accuracy of docking with a new scoring function, effi-

cient optimization, and multithreading. Journal of computational chemistry. 2010;31(2):455-61;PMID: 19499576. Available from: https://doi.org/10.1002/jcc.21334.

20. Kyte J, Doolittle RF. A simple method for displaying the hydropathic character of a protein. Journal of molecular biology. 1982;157(1):105-32;Available from: https://doi.org/10.1016/0022-2836(82)90515-0.